ELSEVIER

Journal of Structural Geology 27 (2005) 1788–1802

JOURNAL OF STRUCTURAL GEOLOGY

www.elsevier.com/locate/jsg

Transpressional deformations at lateral boundaries of propagating thrust-sheets: the example of the Meuse Valley Recess within the Ardennes Variscan fold-and-thrust belt (N France–S Belgium)

F. Lacquement[a,b], O. Averbuch[b,*], J.-L. Mansy[b], R. Szaniawski[b,c], M. Lewandowski[c]

[a]*Bureau de Recherches Géologiques et Minières, 3 Av. C. Guillemin, 45000 Orléans, France*
[b]*Université de Lille 1, Processus et bilans en domaines sédimentaires, UMR 8110, 59655 Villeneuve d'Ascq cédex, France*
[c]*Institute of Geophysics of the Polish Academy of Sciences, Ks. Janusza 64, 01-452 Warsaw, Poland*

Received 17 June 2004; received in revised form 5 April 2005; accepted 8 May 2005
Available online 9 August 2005

Abstract

The 3D kinematics of the fold–thrust structures within the Meuse Valley Recess (MVR) (Ardennes Variscan thrust belt, N France–S Belgium) have been investigated using an integrated approach combining geological mapping, cross-section analyses and studies of magnetic fabrics and paleomagnetic data at a total of 52 sites distributed within the study area. Fold–thrust geometries, strain distribution and thrust-sheet rotational patterns lead to a conceptual structural model illustrating natural deformation processes at lateral boundaries of propagating thrust-sheets. The MVR is shown to result from distributed transpressional deformation of the Ardennes Basal Thrust hanging wall above a buried lateral/oblique ramp inherited from the Lower–Middle Devonian extensional tectonics of the sedimentary wedge. This deep lateral/oblique discontinuity basically controls the thickness and basal friction of the Ardennes thrust wedge, thus resulting in contrasting thrust propagation west and east of the MVR. Out-of-plane strain within the transfer zone includes some varying components of normal-to-bedding shear and lateral shortening depending on the proximity with the buried lateral discontinuity. A gradient of lateral shortening is evidenced towards this discontinuity, thus acting as a buttress zone. We emphasize the high friction conditions prevailing along the lateral borders of the thrust sheets, which potentially result in drag effects during foreland-directed thrust propagation. Such additional shear strain is suggested to be accommodated by late pervasive thrust-sheet rotation and lateral broadening of the deformed zone subsequent to oblique folding close to the lateral/oblique boundary.

Keywords: Fold-and-thrust belt; Lateral/oblique ramp; Transpression; Ardennes; Variscan thrust front

1. Introduction

Lateral boundaries of fold–thrust structures within the outer parts of orogenic belts have been shown to develop complex 3D kinematics resulting in significant structural strike deviation and relatively steeply dipping axial plunges (e.g. Apotria, 1995; Frizon de Lamotte et al., 1995; Wilkerson et al., 2002). On the basis of analog modeling experiments, such along-strike geometrical evolutions have been generally attributed to either displacement gradients due to lateral variations in the strength of the underlying décollement zone or lateral changes in the thickness of the thrust wedge (either combined or in isolation) (Dixon and Liu, 1992; Marshak et al., 1992; Calassou et al., 1993; Philippe, 1995; Macedo and Marshak, 1999; Paulsen and Marshak, 1999). These changes in the mechanical properties of the thrust wedge can be continuous along strike, or be localized to a very narrow domain. The latter situation involves a sharp, steeply dipping discontinuity oriented parallel or oblique to the thrusting direction transferring differential movements between adjacent thrust units having different mechanical behavior, i.e. a lateral/oblique ramp (e.g. Dahlstrom, 1970; Butler, 1982; Schirmer, 1988). Obviously, these lateral changes primarily result from the inherited basin geometry. Basement normal-fault zones coeval with the basin development form strong mechanical

* Corresponding author. Fax: +33 320 43 49 10.
E-mail address: olivier.averbuch@univ-lille1.fr (O. Averbuch).

0191-8141/$ - see front matter © 2005 Elsevier Ltd. All rights reserved.
doi:10.1016/j.jsg.2005.05.017

heterogeneities in the sedimentary wedge and thus have been shown both by modeling experiments and structural studies to control the location of future footwall thrust ramps (Wiltschko and Eastman, 1982; Thomas, 1990; Frizon de Lamotte et al., 1995; Philippe, 1995; Tavarnelli, 1996). Thrust-sheet motion along such lateral/oblique ramp-flat system has been shown to induce variable amounts of out-of-plane strain of the hanging wall block including layer-normal simple shear and lateral/oblique shortening owing to buttressing effect of the ramp (Coward and Potts, 1983; Hyett, 1990; Apotria et al., 1992; Averbuch et al., 1993; Apotria, 1995; Holl and Anastasio, 1995). Within lateral boundaries of thrust-sheets, such a mechanism generally results in distributed transpressional deformation expressed by a complex pattern of fold–faults interaction accommodating thrust-sheet rotation around vertical axes (Apotria, 1995; Allerton, 1998; Bayona et al., 2003), tear faulting (Donzeau et al., 1993) and oblique layer-parallel shortening (Averbuch et al., 1993; Apotria, 1995).

This paper aims to address the problem of 3D kinematics of fold–thrust structures using a multidisciplinary structural study of the Meuse Valley Recess (MVR) within the Ardennes fold-and-thrust belt (N France–S Belgium Variscan thrust front). Fold–thrust geometries, strain distribution and thrust-sheet rotational patterns are investigated using an integrated approach coupling geological mapping, cross-section analyses and studies of magnetic fabrics and paleomagnetic data at a total of 52 sites distributed along the MVR. These data are finally integrated in a structural model illustrating natural deformation processes at lateral boundaries of propagating thrust sheets.

2. The Ardennes fold-and-thrust belt: geological overview

The Ardennes fold-and-thrust belt (N France–S Belgium) represents the northern thrust front of the western European Variscan orogenic belt (Fig. 1a), which resulted from the collision of the Laurentia–Avalonia–Baltica (i.e. Old Red Sandstones Continent) and Gondwana margins in Upper Paleozoic times. It includes non-metamorphic to epimetamorphic sedimentary rocks of mostly Devonian–Carboniferous age (Fig. 2) deposited at the southern border of the 'Old Red Sandstones' continent in a rifted continental margin-type environment (Rheno–Hercynian basin).

Structurally, the N France– S Belgium Variscan thrust front is a composite feature (Fig. 1b) that extends from the Channel–Boulonnais thrust belt (Averbuch et al., 2004) to the Ardennes thrust belt changing progressively strike from NW–SE to NE–SW. This large-scale strike change is accommodated by second-order curved thrust zones, relaying in a complex way within the Western Ardennes fold-and-thrust belt. Such segmentation is exemplified by the map geometry of the 'Midi Thrust Zone' (Mansy et al., 1999), which corresponds to the emergence of the Ardennes Basal Thrust (ABT), a crustal-scale, gently south-dipping décollement zone accommodating a general NNW-directed displacement. The Midi Thrust Zone separates the Ardennes Belt, displaying a classic thrust-wedge geometry from the underthrusted Namurian–Westphalian coal-bearing, foreland basin, heavily dismembered along its southern border (Fig. 1c). This up to 4-km-thick basin lies on top of the Brabant massif basically structured in Caledonian times and surrounded by a reduced Upper Devonian–Carboniferous sedimentary cover. A recent interpretation of a seismic profile across the Western Ardennes belt (Fig. 1c) shows that the minimum total displacement along the basal thrust system is approximately 70 km and that a major part of this displacement occurred by out-of-sequence thrusting after deposition of the Namurian–Westphalian molasse (Lacquement et al., 1999). A pronounced flexure of the underthrust Brabant foreland is visible at the tip of the frontal thrust system resulting from the localized load, coeval with the out-of-sequence thrust stack (Averbuch et al., 2004).

Unlike the Brabant foreland, the Ardennes thrust belt displays a thick Lower Devonian sequence composed of alternating shale and sandstone (Fig. 2). The thick shaly layers at the base of this sequence act as a major décollement level that localized the ABT in its outer part. The general southward increase in thickness of the Devonian–Carboniferous sedimentary sequence and associated facies changes suggest a rifted passive margin type geometry of the Rheno–Hercynian basin (e.g. Meilliez et al., 1991; Franke, 2000; Oncken et al., 2000; Lacquement, 2001). As proposed by Oncken et al. (2000) for the Eastern Ardennes belt, overturned basement-involved thrust sheets (OTS in Fig. 1c) in the footwall of the Midi Thrust Zone are likely to represent the result of the short-cut dissection and transport upon the upper flat of the rift shoulders that formed the northern extension of the Lower Devonian deposits. These structures illustrate the strong segmentation of the basin that in turn controlled the depth and extension of the potential décollement levels within the inverted Variscan belt. Based on depositional facies variations, syn-sedimentary fault zones active during the Lower–Middle Devonian rifting event have been shown to display dominant ENE–WSW and NW–SE trends (Meilliez et al., 1991), i.e. roughly normal and parallel to the Variscan thrusting directions. Therefore, these early structures are likely to have localized the frontal and lateral ramps in the Ardennes thrust wedge.

3. The Meuse Valley Recess: geometry and 3D structural model

Within an about 40-km-wide NW–SE-trending corridor centered on the Meuse river valley, the axial trace of the fold–thrust structures display pronounced strike deviations (Fig. 1b). The general ENE–WSW trend of the Western Ardennes thrust belt (average N070) turns clockwise to a

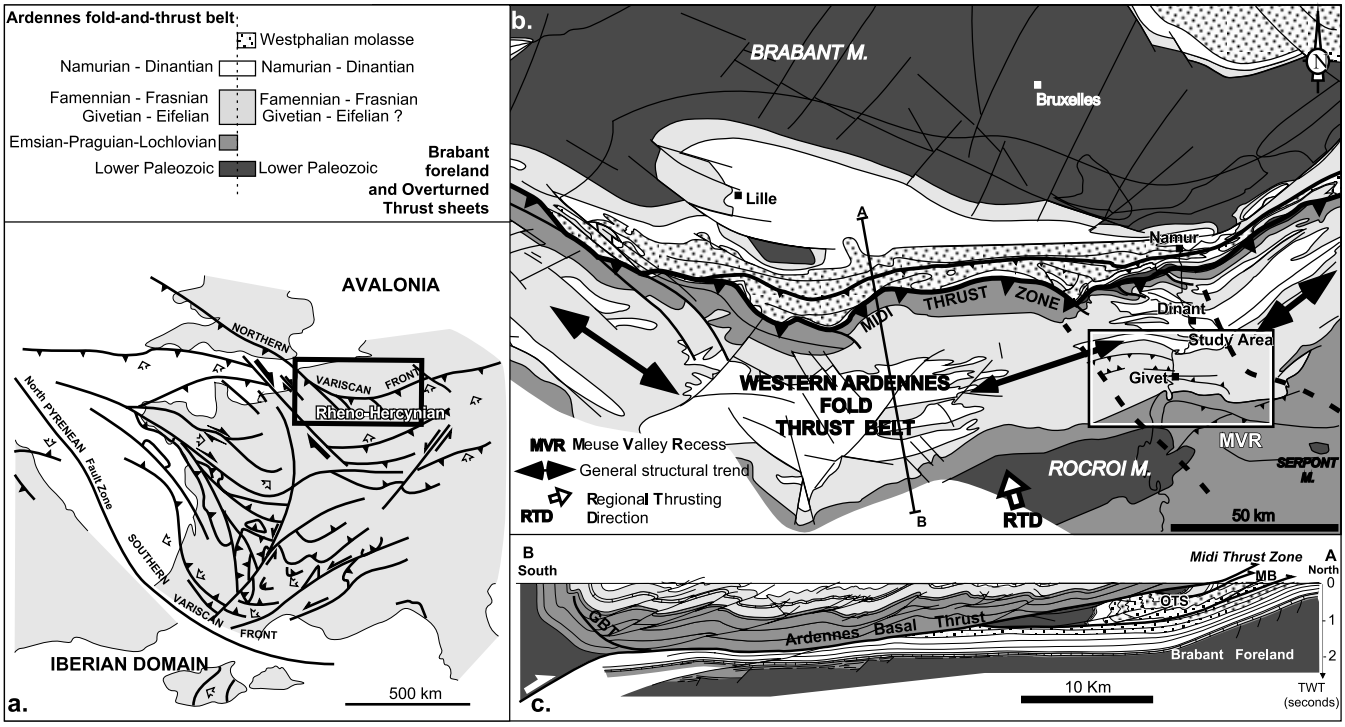

Fig. 1. (a) A tectonic map of the Western European Variscan belt (after Ledru et al., 2001). The rectangle locates the map in (b); (b) Subcrop map of the Northern France–Southern Belgium Variscan thrust front. The borders of the Meuse Valley Recess are emphasized by dashed lines. The specific study area is shown by a rectangle (map of Fig. 3). Section A–B refers to the M146 seismic line presented in (c); (c) A seismic cross-section (M146 profile) through the Western Ardennes thrust belt; OTS, Overturned thrust sheets; MB, Molassic basin; note the classical thrust wedge geometry of the Ardennes thrust belt upon a crustal scale S-dipping basal thrust.

WNW–ESE trend in the center of the corridor then turns back to a NE–SW trend towards the Eastern Ardennes belt (average N050). This progressive change in structural trend draws a concave-toward-the-foreland curvature defined here as the Meuse Valley Recess (MVR).

This strike deviation is particularly well represented within the southern part of the Ardennes thrust belt (Fig. 3). This zone corresponds to the northern forelimb of a major basement culmination (the Rocroi culmination) (Fig. 1b), which exposes in its core, a thick turbiditic series of Cambrian–Ordovician age submitted to very low grade metamorphism. This culmination can be interpreted as a large thrust-related anticlinal stack developed above a major footwall ramp of the ABT (Fig. 1c). North-northwestward displacement is transferred towards the foreland upon the base Lower Devonian décollement zone gently dipping to the south. The forelimb of the Rocroi culmination includes a thick Devonian–Carboniferous cover with a general steep northern dip (see the geological map of Fig. 3 and the cross-sections of Fig. 4). In the Givet area, it is affected by a complex out-of-the-syncline backthrust zone, the Givet backthrust zone (GBT) that roots at depth onto the ABT. It climbs southward through the Devonian series and emerges within the thick Frasnian–Famennian shaly layers situated just at the forelimb synclinal hinge. Due to the particularly weak behavior of the Frasnian–Famennian sequence, which potentially acts as a roof décollement level, displacement along the GBT is distributed into subsidiary thrusts and accommodated by intense folding and internal deformation.

From a structural point of view, two very different domains can be defined on both sides of the GBT (Lacquement, 2001): (1) the southern one corresponds to the steep forelimb of the Rocroi basement anticline, which involves the Lower–Middle Devonian series. This general north-dipping limb includes numerous second-order north-verging recumbent folds that display gently south-dipping axial plane cleavage. Folds are systematically dissected by NNW-verging forelimb thrusts indicating a general top-to-the-north simple shear of the fold–thrust structures; (2) north of the GBT, structures are characterized by polyharmonic upright folds with sub-vertical pressure-solution cleavage. This deformation pattern indicates bulk pure shear and layer-parallel shortening of the Upper Devonian–Carboniferous cover likely to be the result of a buttressing effect in front of the North-northwestward propagating Rocroi thrust-sheet (Fig. 4, sections a–c.).

Likewise, within the MVR, deformation is strongly heterogeneous, and strike-changes are accommodated in different ways, depending on their location with respect to the GBT. South of the GBT, the 400-m-thick competent Givetian limestone unit is involved in an about 50-km-wide oblique limb developed at the lateral tips of thrusts cross-cutting the Rocroi basement anticline and its Lower Devonian cover (Figs. 3 and 4). This large oblique

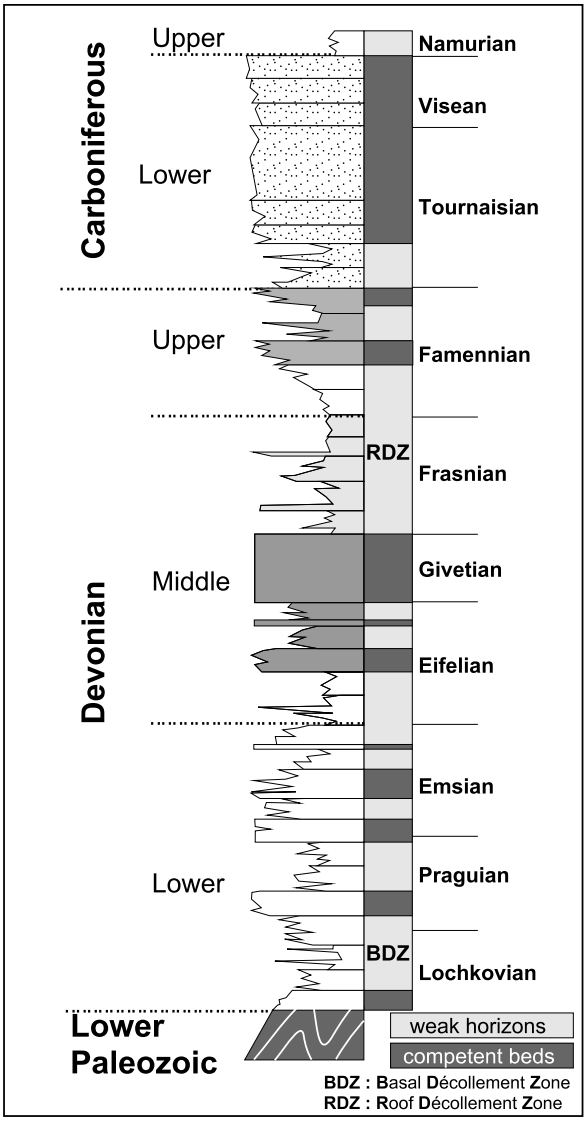

Fig. 2. Stratigraphy and rheological properties of Devonian–Carboniferous rocks involved in the Ardennes thrust belt. Note the existence of two main décollement-zones in the thrust wedge: a basal one within the Lochkovian shales and an upper one within the Frasnian–Famennian shales.

culmination wall is affected by kilometer-scale minor folds exhibiting a gradual increase in axial plunge (from 5 to about 50°) towards the inner parts of the MVR. Increase in the plunge of fold axes is associated with a progressive clockwise deviation of their strike (up to about 70°) (Fig. 3). An interesting point to be noticed is that the area of both maximum axial plunges and strike deviation is not located in the center of the corridor but is offset towards its eastern boundary. As proposed by Wilkerson et al. (2002) on the basis of ramp-related fold modeling, such high plunges and strong deviations of fold terminations suggest the existence of a buried lateral/oblique ramp beneath the inner parts of the strike-deviated corridor. Alternatively, the oblique culmination wall displays in specific deformation zones a significant cleavage tilt either towards the NNE or towards the E (Fig. 3). Like fold axial plunge, the amplitude of cleavage tilt within these zones globally increases towards the east. However, it is worth noting that areas of tilted cleavage are restricted to the central part of the oblique culmination wall and are not observed in the easternmost part of the MVR.

Within the Frasnian–Famennian sequence involved in the large syncline at the roof of the GBT, deformation is characterized by approximately 10 km scale en-échelon folds (Fig. 3). These folds are closely related to steep subsidiary back-thrusts branching on the GBT (see cross-sections in Fig. 4). Towards the north, the amplitude of such folds gradually decreases, indicating a general strain gradient towards the GBT. These second-order folds fade out northwards and the major fold structures display gently curved axes in the northern part of the study area.

Beneath the MVR, the geometry at depth can be constrained using both deep boreholes (the Focant and Rosée boreholes; see location in Fig. 3) (Boulvain and Coen-Aubert, 1997; Han et al., 2003) and a set of previously published seismic profiles from the Famenne area (e.g. Raoult, 1986; Goudalier, 1998), along the eastern boundary of the recess (the inner zones). The Focant borehole is particularly interesting because it is situated in the inner zones of the strike-deviated corridor, a few hundred meters north of the GBT emergence. As shown on cross-section (c) in Fig. 4, the Focant borehole surprisingly encountered 3000 m of strongly deformed Frasnian series (e.g. Raoult, 1986), which usually have thicknesses of about 400 m. This geometry has been interpreted as the result of the existence of a very deep and tight syncline bordered by sub-vertical limbs and dissected by numerous thrust faults. The GBT is encountered at about 2000 m showing its global sub-vertical attitude (i.e. parallel to the oblique wall of the Rocroi culmination). An E–W seismic profile through the GBT within the eastern part of the deformed corridor (Goudalier, 1998) suggests that this thrust branches rapidly laterally onto the ABT cutting through the Givetian limestone unit involved in an apparent westward thrusting (cross-section (d) in Fig. 4). This geometry points to a significant component of shortening at high angle to the regional thrusting direction inducing the upward lateral expulsion of a restricted thrust sheet in the innermost zone of the MVR.

On the other hand, previous interpretations of the network of N–S and E–W seismic profiles within the eastern part of the Meuse valley recess help to further constrain the deep geometry of the ABT as well as the structure of the ABT footwall units. As shown by Raoult (1986), seismic depth maps of the well-resolved ABT reflector display strong lateral variations from west to east in the investigated area (Fig. 5). The ABT lies at about 2.5 s two way time travel (TWT) in the central part of the recess (about 7–8 km depth following classical seismic velocity values within the Ardennes belt (Lacquement, 1997)) and climbs progressively eastward to about 1.8 s TWT east of the recess (about 5 km depth as shown by the Havelange

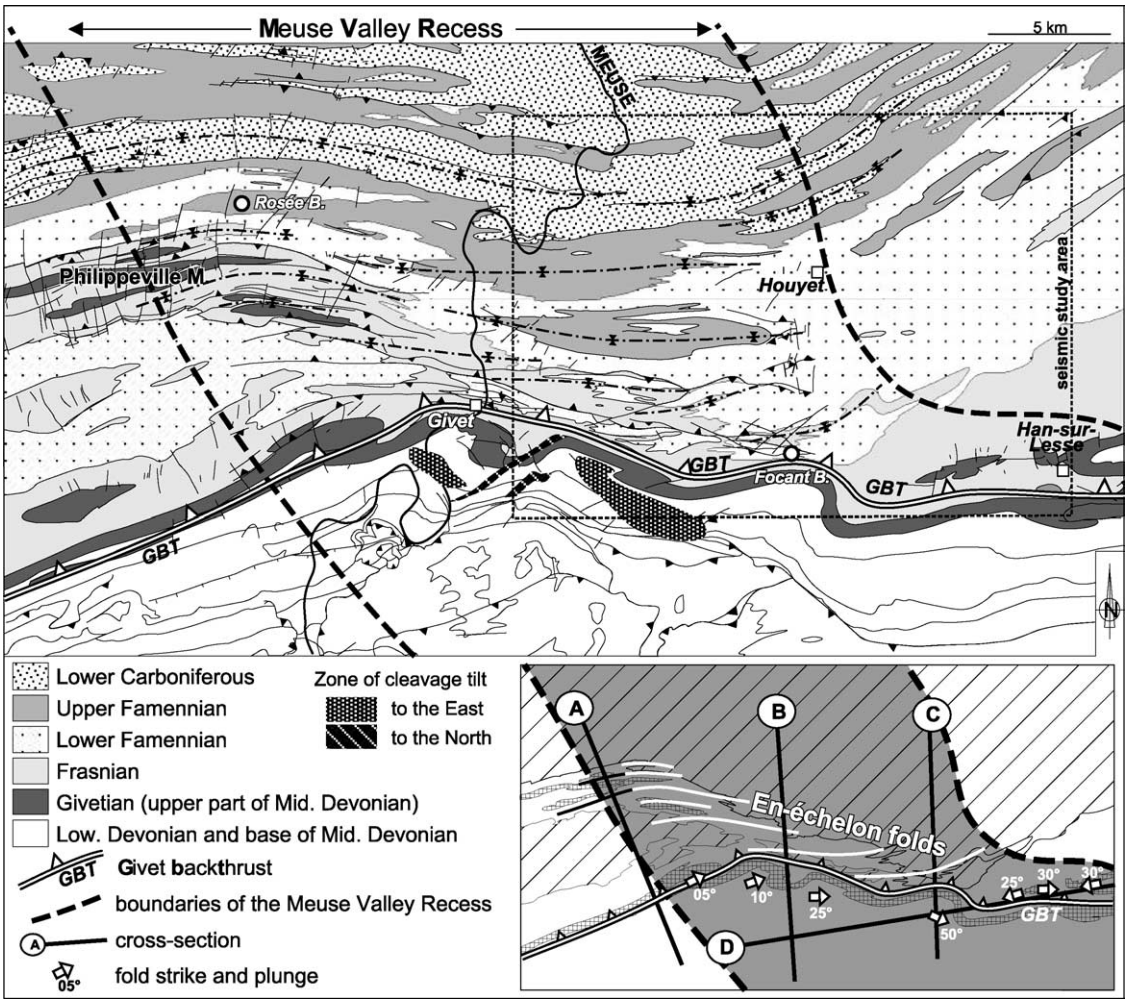

Fig. 3. (a) Geological map of the northern forelimb of the Rocroi basement culmination along the Meuse river valley. Note the progressive structural strike deviation characteristic of the Meuse Valley Recess (MVR) and also the existence of a significant back-thrust zone (GBT) along the Givetian limestone unit involved in the culmination wall. The zones of occurrence of cleavage tilt are reported on the map. Note the locations of the Focant and Rosée deep boreholes. (b) A schematic structural map of the study area showing the fold geometries along the MVR, and localizing the cross-sections of Fig. 4. Note the increase in fold strike deviation and plunges (up to 50°) towards the inner parts of the recess.

deep borehole (Raoult, 1986)). The interpreted seismic depth isovalues present a general NW–SE trend, almost parallel to the boundary of the corridor but slightly oblique to the regional thrusting direction. Moreover, these variations roughly parallel the lateral changes of the depth of a prominent reflector in the footwall of the ABT (the Y reflector of Raoult (1986) supposed to be the top of the Lower Paleozoic basement). Despite the relatively low resolution of the 3D seismic data, this geometric pattern shows that the structural strike variations observed in the Devonian–Carboniferous cover within the MVR are localized by a pronounced lateral step in the depth of the ABT. It forms a major buried lateral/oblique ramp in the thrust wedge as exemplified by cross-section (d) in Fig. 4, perpendicular to the regional thrusting direction. As shown on the large-scale map of Fig. 1, this lateral ramp clearly limits the eastward extension of the Rocroi basement culmination, thus decoupling two major thrust units, west and east of the MVR. Therefore, the MVR can be considered as the distributed hanging wall signature of a buried transfer zone between the Western and Eastern Ardennes thrust sheets. The seismic data moreover suggest that this lateral/oblique ramp is controlled by the ABT footwall topography, i.e. the geometry of the Brabant substratum. Considering the highly segmented nature of the Ardennes thrust wedge, the most satisfactory explanation for such basement topography is the existence, at depth, of a regional syn-sedimentary fault zone, inherited from the Devonian basin development (see the sketch 3D structural model presented in Fig. 5).

4. Magnetic fabric analysis

To further document the strain pattern within the MVR, we carried out a magnetic fabric analysis on 35 sites

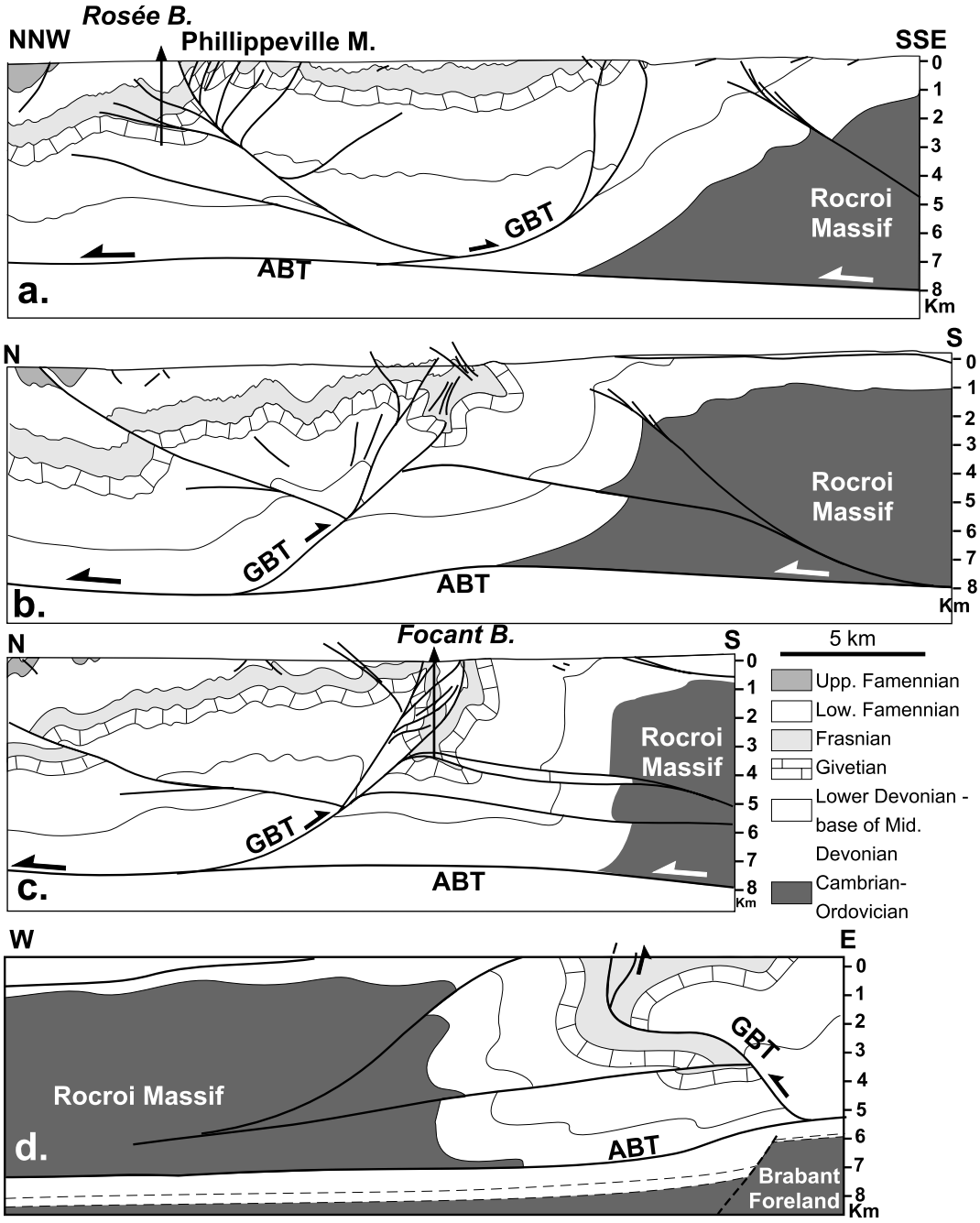

Fig. 4. Cross-sections through the forelimb of the Rocroi culmination: (a) parallel to the regional thrusting direction (RTD); (b) and (c) oblique to RTD; (d) perpendicular to RTD. See locations in Fig. 3b.

distributed within the structure. This method, based on the analysis of the anisotropy of the magnetic susceptibility (AMS), has been widely shown to represent a semi-quantitative strain indicator (see reviews in Tarling and Hrouda (1993) and Borradaile and Henry (1997)), particularly efficient in weakly deformed areas, such as foreland fold-and-thrust belts where few strain markers are available (Averbuch et al., 1992; Parès et al., 1999). AMS reflects the preferred orientation of grains and/or crystal lattices of all the minerals that contribute to the magnetic susceptibility (essentially ferro- and paramagnetic minerals). It can be described by an ellipsoid characterized by the orientation and the relative magnitude of three principal axes, a maximum axis, K_{max}, an intermediate axis K_{int} and a minimum axis K_{min}. The shape of the ellipsoid is described by the AMS shape parameter T (Jelinek, 1981), with $0 < T \leq 1.0$ for oblate ellipsoids (dominantly planar fabrics) and $-1.0 \leq T < 0$ for prolate ellipsoids (dominantly linear fabrics) (Fig. 6). Strength of anisotropy is described by the anisotropy degree P (see Jelinek, 1981) (Fig. 6).

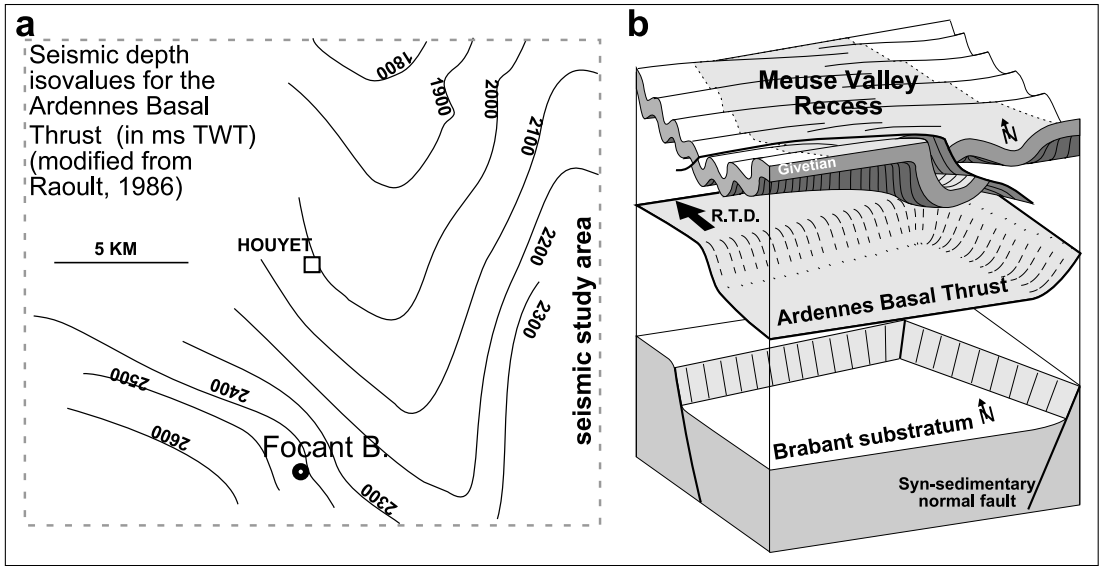

Fig. 5. (a) Seismic depth isovalues (in milliseconds two way time travel (TWT)) for the Ardennes Basal Thrust (ABT) along the eastern part of the Meuse Valley Recess (MVR) (modified from Raoult, 1986). Note the pronounced NW–SE-trending step in the depth of the ABT. (b) A 3D sketch structural model showing the close relationships between the MVR within the Ardennes thrust belt and the lateral variations in the geometry of the Ardennes basal thrust. Note that the buried lateral/oblique ramp localizing the MVR is controlled by the basement topography inherited from the Rheno–Hercynian basin development.

To provide the best possible distribution within the structure, sites having different lithologies (carbonates, shales and sandstones, except for red beds) and age (Praguian to Famennian) were sampled (see sample distribution in Fig. 7). The site-mean magnetic susceptibilities (K_m) are globally low (below 500×10^{-6} SI) (Fig. 6a) indicating a potentially combined paramagnetic (clay minerals) and ferromagnetic (iron oxides or sulfides) source for the magnetic anisotropy. Site-mean anisotropy degrees (P_m) are also globally low (below 1.15) indicating

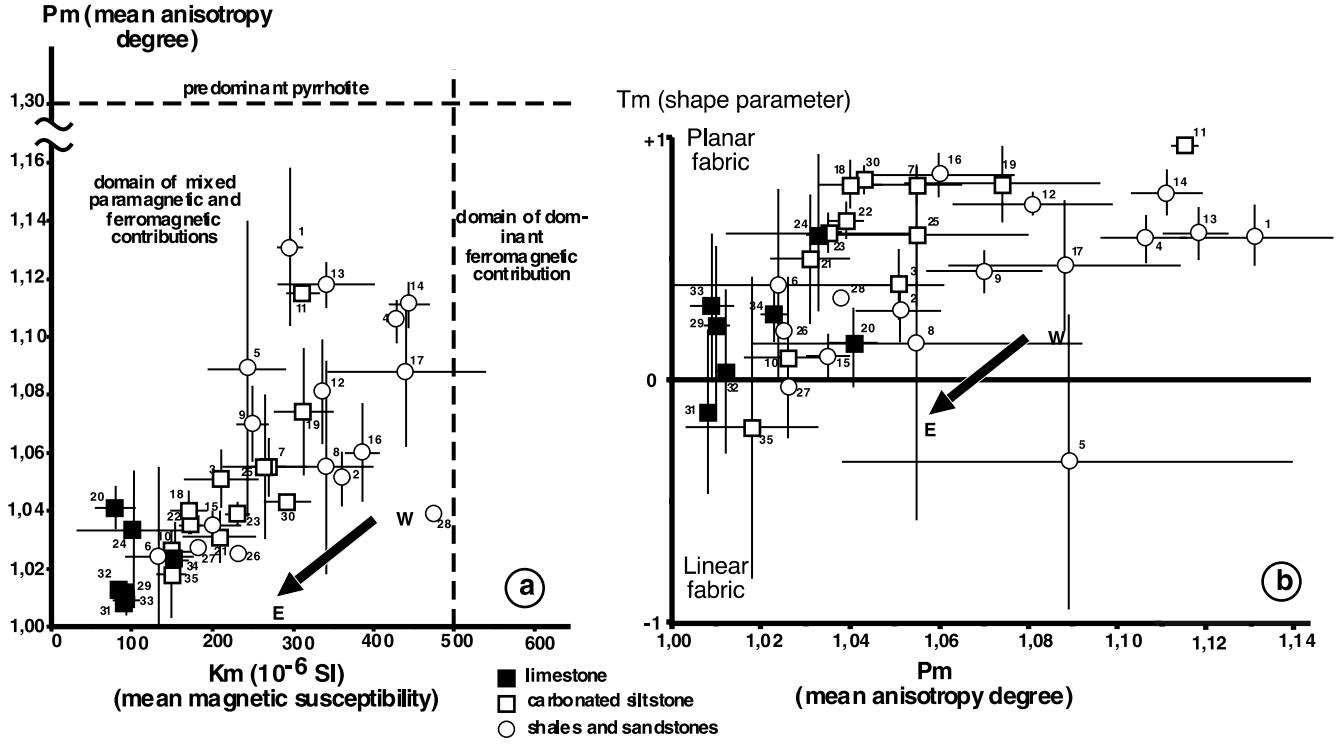

Fig. 6. Evolution of site-mean parameters of the anisotropy of magnetic susceptibility (AMS) along the Meuse Valley Recess. Numbers refer to sampling sites located in Fig. 7. (a) Diagram reporting the anisotropy degree P_m versus magnetic susceptibility K_m. (b) Diagram reporting the AMS shape parameter T_m versus the anisotropy degree P_m.

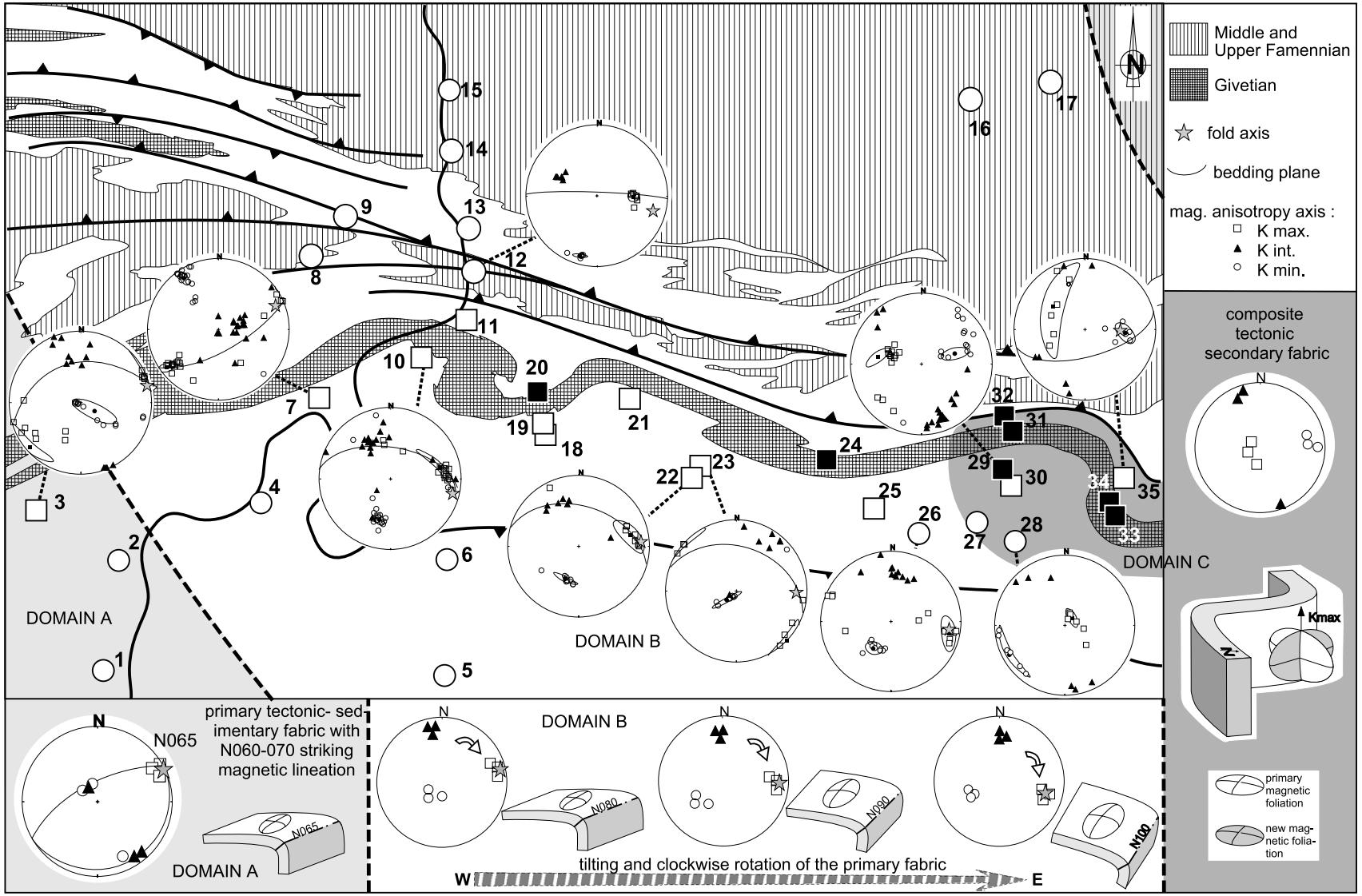

Fig. 7. Sketch geological map with the location of sites sampled for the magnetic fabric analysis (black squares refer to limestones, white squares to calcareous shales and white circle to shales and sandstones). The stereoplots (lower hemisphere, equal area) show the orientation of principal axes of the ellipsoid of anisotropy of magnetic susceptibility for representative sites along the Meuse Valley Recess. Black squares correspond to the orientation of the tensorial mean maximum axis K_{max} and black circles to the tensorial mean minimum axis K_{min}. Ellipses correspond to the confidence angles around the mean directions. Note the progressive evolution of the magnetic fabric from west (domain A) to east (domain C). See explanations in text.

that ferromagnetic iron sulfides (pyrrhotite) do not contribute significantly to the AMS (Rochette et al., 1992; Robion et al., 1999). Alternatively, the somewhat reducing conditions associated with the dark gray to green color of sampled shales and sandstones (we avoided red beds in sampling) suggest that magnetite and clays form the dominant contributions to the magnetic anisotropy. A combination of magnetite grain shapes and phyllosilicate crystallographic preferred orientations is thus likely to be responsible for the bulk magnetic anisotropy. Contrasting rheological properties of studied rocks, as well as the relative amounts of both these contributions to the sampling set, induce significant variations of the mean magnetic susceptibilities and anisotropy degrees. Shaly and sandy rocks have susceptibilities and anisotropies significantly higher than carbonate-bearing rocks (Fig. 6a). The global correlation of magnetic susceptibility and degree of anisotropy exemplifies the control exerted by the lithology and the magnetic mineralogy on the AMS (Rochette et al., 1992). If we consider, however, dominant lithologies separately, it is worth noting the persistence of significant variations of the anisotropy degree that can be related to the structural position of the sampled site (Figs. 6 and 7). Sites from the most deformed zone of the recess (the eastern sites of our distribution) display surprisingly low anisotropies compared with sites located outside the MVR or towards more external parts (the western sites of our distribution).

Site-mean shape parameters, T_m (Fig. 6b) display the same type of distribution with a significant structurally-related evolution from strongly planar to slightly linear fabrics. This evolution correlates well with the anisotropy degree showing that the most anisotropic fabrics from the western zones are dominantly planar, whereas the less anisotropic fabrics from the inner zone of the MVR are triaxial or slightly linear. As frequently observed in complex tectonic zones, this paradox suggests the composite nature of magnetic fabrics observed in the inner zone, owing to the superimposition of two non-coaxial planar sub-fabrics (Housen et al., 1993; Parés et al., 1999; Robion et al., 1999).

The orientation of principal axes of magnetic susceptibility corroborates this interpretation. Outside the MVR (domain A in Fig. 7), classical fabrics from foreland fold-and-thrust belts can be observed: K_{min} axes are clustering along the bedding-pole (or sometimes along the cleavage pole, depending on the lithology). Within this magnetic foliation, maximum susceptibility axes (magnetic lineation) cluster horizontally parallel to the fold axis (at the outcrop-scale, the cleavage–bedding intersection), here about N060–N070. This common type of fabric has been largely shown to result from the interference between growing pressure-solution cleavage surfaces and inherited bedding planes (Borradaile and Tarling, 1981; Kligfield et al., 1981; Averbuch et al., 1995; Parés et al., 1999). In these zones, magnetic fabrics thus evidence a shortening oriented about N330–340, i.e. parallel to the average thrusting direction. Such a type of fabric is also characteristic of the outer parts of the MVR (domain B in Fig. 7); it is worth noting, however, that with alike fold axes, the magnetic lineations tend to plunge eastward and progressively deviate towards an E–W to NW–SE direction.

In the easternmost part of the MVR (domain C in Fig. 7), the fabric is completely different from the other parts of the Ardennes belt. Regardless of the bedding attitude, a steep magnetic foliation striking about NNW–SSE to N–S can be observed. It is associated with a sub-vertical to steeply dipping magnetic lineation. As suggested by their low anisotropy degrees and slightly linear character, these fabrics have likely been reworked by superimposition of an incipient NNW–SSE tectonic foliation upon the primary tectonic–sedimentary fabric of type similar to those observed in other parts of the belt (Fig. 7). The sub-vertical magnetic lineation would thus correspond to the intersection between these two vertical foliations. Such a late NNW–SSE penetrative tectonic foliation implies a WSW–ENE shortening, i.e. a lateral shortening normal to the general thrusting direction. This lateral shortening is mostly localized within the eastern part of the MVR, as is also demonstrated by the Famenne seismic sections. In the more external parts, as also evidenced by the specific occurrence of zones of cleavage tilt (Fig. 3), out-of-plane deformation is expressed by the tilting and deviation of the initial fabric without any strong penetrative reworking (domain B in Fig. 7).

5. Rotational behavior of thrust-sheets

To constrain the rotational behavior of the tectonic units under study, we made a synthesis of up-to-date paleomagnetic data from the Ardennes thrust belt. Numerous recent paleomagnetic data are available in the Meuse Valley region (Molina Garza and Zijderveld, 1996; Marton et al., 2000; Szaniawski et al., 2003; Zegers et al., 2003) because it provides a natural cross-section through the folded Paleozoic series of the northern Variscan thrust front. Sites with contrasted deviated strike have thus been preferentially analyzed. Although fewer sites with the classical Ardenno–Rhenish ENE–WSW trend have been investigated, there are, however, sufficient data to discuss possible relative rotations associated with the MVR development (Szaniawski et al., 2003). The paleomagnetic sites distribution is reported in Fig. 8. Magnetite-bearing limestones of Middle Devonian and Carboniferous age are dominantly represented in the data set because they have been shown to display remanent magnetizations more stable than Lower or Upper Devonian red–green sandstones or siltstones. These whole sites have been shown to be remagnetized at different episodes of the deformation process but always with a reverse polarity (Kyaman superchron) (Szaniawski et al., 2003). Incremental untilting test procedures in different regional folds have evidenced a high temperature remagnetization component to occur at the incipient stages of folding probably due to the burial of

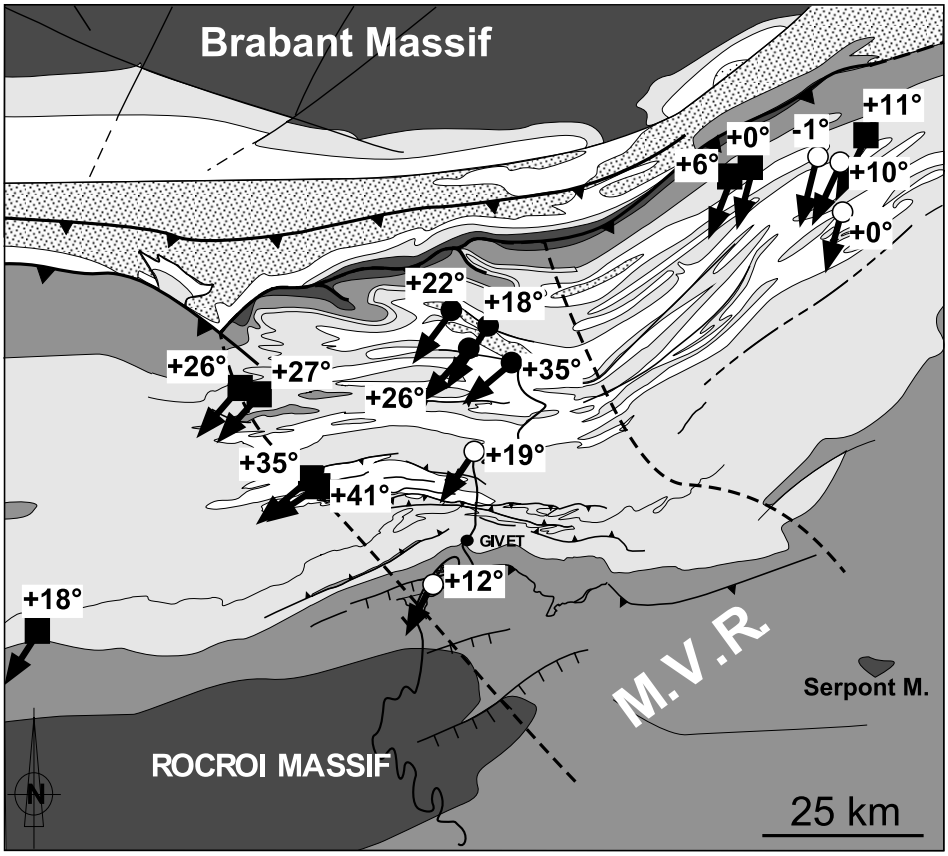

Fig. 8. Paleomagnetic results from relevant published sites within the Ardennes thrust belt (same geological map legend as Fig. 1). Black circles refer to paleomagnetic data from Molina Garza and Zijderveld (1996), white circles to data from Szaniawsky et al. (2003) and black squares to data from Zegers et al. (2003). The arrow corresponds for the majority of sites to the measured declination of the HT component of the remanent magnetization of some Givetian and Carboniferous limestones. For the few sites in Devonian siliciclastics, the arrow corresponds to the measured declination of the characteristic remanent magnetization (see text for discussion). Numbers correspond to the deviations with the expected declination for the Ardennes thrust belt based on the Westphalian paleopole for the stable 'Old Red Sandstones' continent of Van der Voo (1993).

sedimentary rocks under the thick molassic foreland basin of Namurian–Westphalian age. This remagnetization event occurred before most of the compressive deformation proceeded. Rotations around the vertical axis of the thrust sheets involved in the MVR are thus expected to have been recorded by the deviations of the site-mean remanence declinations with respect to that expected for the stable domain of the 'Old Red Sandstones continent' (here N195 following the Wespthalian paleopole of Van der Voo (1993)). Such an interpretation is not so evident for the Lower Devonian red beds from the southern part of the belt, within the forelimb of the Rocroi massif (Fig. 8), because they display syn- to post-folding remagnetizations. Nevertheless, we calculated the declination deviations for 17 published relevant sites distributed along the Ardennes thrust belt based on previous paleomagnetic studies of Molina-Garza and Zijderveld (1996), Zegers et al. (2003) and Szaniawski et al. (2003). Declination directions along with their deviations to the expected data are reported on a Variscan subcrop tectonic map in Fig. 8. Regardless of the age of the magnetization, these data show a permanent clockwise rotation of strike deviated sites from the MVR compared with zones showing the general trend of the Ardenno–Rhenish segment. The quantitative relationship between the amount of rotation and the local strike deviation at the study site compared with an average reference strike of N060E is plotted in Fig. 9. A clear linear correlation with a slope of 1 can be suggested for sites having strike deviation up to about 35°, indicating the pure rotational origin (orocline type) of the curvature. For sites having strikes deviated more than 35°, rotation does not increase more than about 30–40°. This suggests that rotation around vertical axes, particularly for zones of important strike deviation, does not account for the entire curvature. Instead, rotation increases some previous strike-deviated structures developed as oblique folds at the lateral boundary of the propagating Western Ardennes thrust-sheet.

6. A model for the development of the Meuse Valley Recess

Structural data presented above allow discussion of

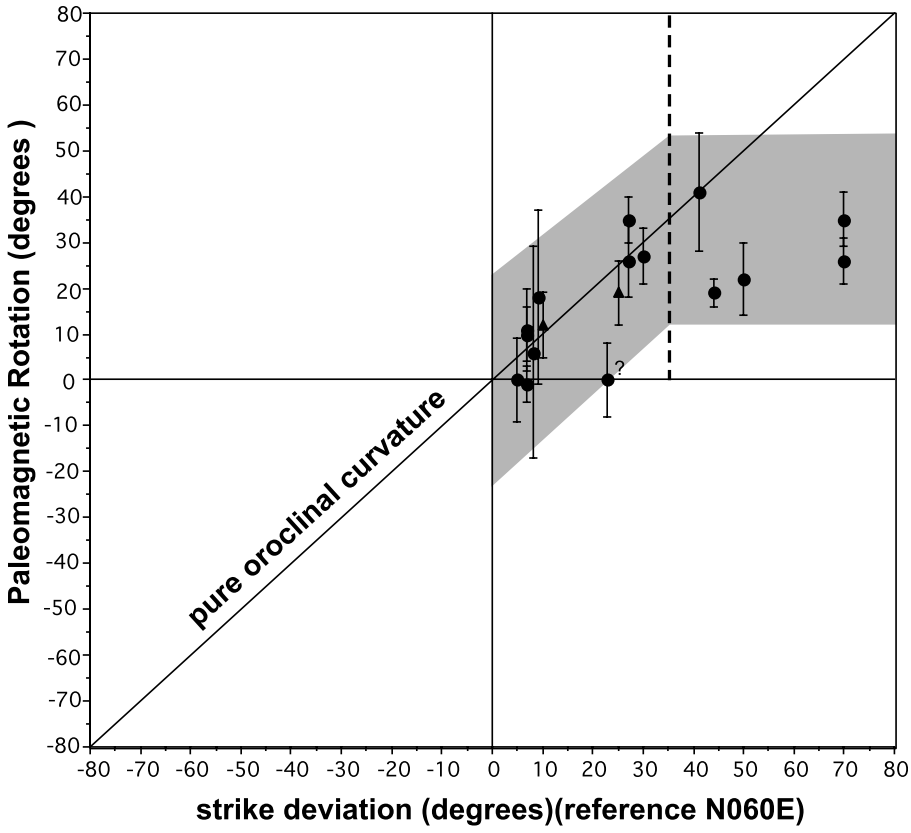

Fig. 9. Diagram showing the paleomagnetic rotation (deviation of declination) versus the strike deviation considering a reference strike of N060E. Black circles: Givetian and Carboniferous limestones; black triangles: Devonian siliciclastics.

geometrical and deformational features associated with the development of the MVR. One of the main results of our 3D structural analysis is that the MVR developed above a deep-seated lateral/oblique ramp controlling changes in the depth of the ABT. About 2 km of vertical offset can be suggested from west to east of the recess based on the roughly depth-converted seismic data. The data, however, do not have enough resolution and geographic coverage necessary to precisely define the geometry of this lateral step. It is unlikely that the 2 km offset would be accommodated by a single lateral/oblique ramp as shown on our simplified model in Fig. 5. Complex relay zones are likely, but are impossible to precisely define at depth. Despite this relatively low resolution, seismic data clearly show that the structure is mould on the basement topography, thus illustrating the control of the basin's early geometry on the thrust wedge development. As suggested by the occurrence of numerous syn-sedimentary normal faults controlling facies changes in the study area (Meilliez et al., 1991), the buried lateral ramp beneath the MVR is likely to be localized by a network of basement fault zones inherited from the Lower Devonian Rheno—Hercynian rifting event. These data thus corroborate observations by Hollmann and Von Winterfeld (1999) in the Western Rhenish massif, east of the Ardennes thrust belt.

A direct consequence of this geometry is that the belt involves a much thicker sedimentary sequence in the Western Ardennes area compared with the Eastern Ardennes which, as it has been shown by analog modeling experiments (e.g. Liu Huiqi et al., 1992; Marshak et al., 1992; Philippe, 1995), results in differential thrust propagation onto the foreland and thrust spacing within the wedge. Moreover, the increased thickness of the Lower Devonian shales at the base of the wedge, combined with enhanced pore-fluid pressure along the décollement zone due to increased overburden thickness are likely to decrease the friction at the base of the Western Ardennes thrust wedge compared with that in the Eastern Ardennes area (Henry and Le Pichon, 1991; Cobbold et al., 2001). Both mechanisms can combine to produce differential thrusting and thrust propagation, west and east of the Meuse Valley Recess. Regardless of its origin, this lateral variation in thrusting should result, in the hanging wall of the Ardennes basal thrust, in a somewhat distributed component of normal-to-bedding simple shear within the transfer zone. Moreover, as suggested by Hyett (1990) and Dixon and Liu (1992), additional shear strain may arise from drag effects against the lateral/oblique boundary during thrust propagation.

Paleomagnetic data within the MVR show that distributed thrust-sheet rotation account for only part of this deformation process. In the zones of maximum fold-strike

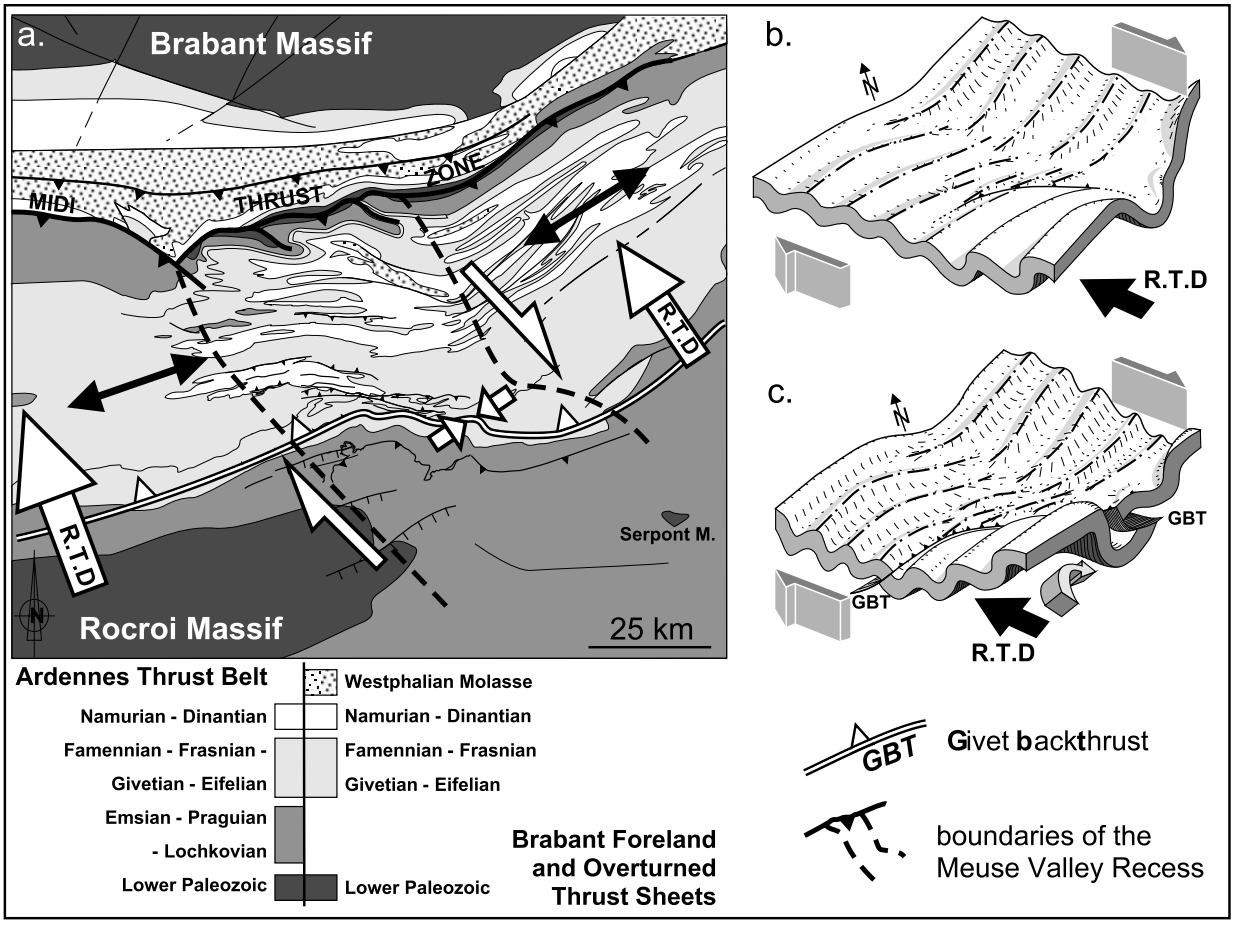

Fig. 10. (a) Structural map showing the kinematics of the Meuse valley transfer zone between the Western and Eastern Ardennes thrust belt. (b) and (c) A 3D model exemplifying the kinematics of deformation at the lateral boundaries of thrust sheets based on the Meuse Valley Recess development. (b) Oblique folding of the Ardennes basal thrust hanging wall above the buried lateral/oblique ramp. (c) Increase of lateral shortening against the lateral discontinuity (buttress effect) and late pervasive thrust-sheet rotation accommodating enhanced shear strain during basal thrust propagation. Note the outward propagation of the transfer zone with increased displacement towards the foreland.

deviation (up to 70°), paleomagnetic data record a maximum of 30–40° clockwise rotation around vertical axes compared with structural domains outside the recess. Conversely, zones which deviate less than 30° from the regional strike display almost pure rotational behaviour (Fig. 9). These data thus show that hanging wall structures situated in the direct vicinity of the lateral/oblique ramp (the eastern part of the MVR) originated as oblique folds (Fig. 10b) that rotated subsequently clockwise as shear strain increased with the propagation of displacement towards the foreland (Fig. 10c). It is worth noting that the width of the strike-deviated zone should have increased during this late process as suggested by the pure rotational behavior of domains deviated less than 30°. This point is corroborated by the occurrence of localized zones of tilt of the early pressure-solution cleavage that are geographically restricted to the external parts of the MVR. The clear asymmetric character of strains within the Meuse Valley corridor show that shear strain propagated dominantly westward along the MVR (i.e. in the direction opposite to that of the buried lateral discontinuity). This deformation scenario is in good agreement with previous strain studies on oblique fold–thrust structures, such as the Wyoming Salient, USA, where rotation was the stage of deformation latest recorded (Apotria, 1995). It moreover satisfies the results of theoretical analytical modeling along transverse zones in thrust belts suggesting the progressive rotation of obliquely-initiated folds towards the orientation of the underlying lateral/oblique discontinuity (Philippe, 1995).

Along the MVR, the component of shortening oblique to the regional top-to-NNW thrusting direction is strongly heterogeneous depending on the rheological properties of deformed units. Thick shaly layers (Frasnian–Famennian unit) develop an en-échelon fold pattern, whereas the competent Givetian limestone unit deforms in a wide oblique culmination wall affected by second-order folds. Decoupling of both mechanical units is accommodated by a complex backthrust zone (the Givet Backthrust Zone). In the inner parts of the MVR, these whole folds exhibit a progressive axial plunge increase up to 50° and displacement along the oblique backthrust zone increases (Fig. 10c). Accordingly, magnetic fabric analyses show a strain

evolution towards inner zones of the MVR characterized by the progressive superimposition of a sub-vertical, broadly NNW–SSE-trending, cleavage plane upon the classical fold-type magnetic fabric characteristic of the general Ardennes fold-and-thrust-belt. Elsewhere in the MVR, the magnetic fabric and the initial pressure-solution cleavage are tilted and deviated with respect to their regional orientation without any significant reworking. The incipient vertical cleavage responsible for the magnetic fabric reworking document an ENE–WSW contraction episode localized predominantly along the eastern border of the MVR. Along with the increase in displacement along the Givet Backthrust Zone, these data demonstrate the presence of a gradient of lateral/oblique shortening towards the area localizing the major lateral discontinuity at depth (Fig. 10). The latter thus clearly acted as a buttress at the lateral boundary separating the Western and Eastern Ardennes foreland propagating thrust sheets.

7. Conclusions

Data presented above illustrate the complex 3D fold–thrust pattern at lateral boundaries of thrust sheets. The MVR results from the distributed transpressional deformation of the ABT hanging wall above a buried lateral/oblique ramp. The ramp acted as a transfer zone between two major NNW-directed thrust sheets of different thickness and having possibly varying basal friction. The resultant out-of-plane deformation includes some heterogeneous components of normal-to-bedding shear and lateral shortening, depending on the structural position within the recess. Normal-to-bedding shear is distributed within the MVR, whereas lateral shortening predominantly occurs along its eastern border, which localizes the deep-seated lateral/oblique discontinuity. Along the MVR, shear strain is expressed by distributed rotation of hanging wall folds with no significant trace of tear faulting. Thrust-sheet rotation around vertical axes does not account, however, for the total strike deviation. In the inner zone of the recess, only about 50% of the strike deviation (about 30–40°) is accommodated by thrust-sheet rotation, the remaining part resulting from initial oblique folding. Thrust-sheet rotation thus appears as a late effect of shear strain during differential thrust propagation. The pure rotational origin of strike deviation within the outer zones (sites deviated less than 30°) as well as the tilting of early strain markers suggest that the transfer zone broadened and propagated laterally outward (i.e. towards the west) during ongoing foreland-directed thrusting. Alternatively, lateral shortening clearly increases towards the eastern border of the MVR. The zone localizing the deep lateral discontinuity thus acted as a buttress likely due to edge effects against the buried lateral/oblique ramp. During propagation of thrusting, our data analysis thus emphasizes the high friction conditions prevailing along the lateral/oblique transfer zone. Drag effects along this discontinuity are therefore very likely with increased displacement along the basal thrust zone. Such a mechanism would result in enhanced shear strain that could account for the late thrust sheet rotation of the hanging wall folds and lateral outward broadening of the transfer zone.

Acknowledgements

This work has been conducted during the PhD theses of F.L. and R.S. at the University of Lille 1. It is a contribution of the 'Atelier Nord' of the UMR CNRS 8110 and of the Institute of Geophysics of the Polish Academy of Sciences. Additional financial support has been provided by the Bureau de Recherches Géologiques et Minières (France geological map project, P. Rossi coord.). We thank B. Vendeville and D. Frizon de Lamotte for friendly reviews of an early version of the text. The two journal reviewers, Y. Philippe and D. Wiltschko, are greatly thanked for their constructive remarks that strongly improved the previous version of this article.

References

Allerton, S., 1998. Geometry and kinematics of vertical-axis rotations in fold and thrust belts. Tectonophysics 299, 15–30.

Apotria, T.G., 1995. Thrust sheet rotation and out-of-plane strains associated with oblique ramps: an example from the Wyoming salient, USA. Journal of Structural Geology 17, 647–662.

Apotria, T.G., Snedden, W.T., Spang, J.H., Wiltscko, D.V., 1992. Kinematic models of deformation at an oblique ramp. In: McClay, K. R. (Ed.), Thrust Tectonics. Chapman and Hall, London, pp. 141–154.

Averbuch, O., Frizon de Lamotte, D., Kissel, C., 1992. Magnetic fabric as a structural indicator of the deformation path within a fold–thrust structure: a test case from the Corbières (NE Pyrenees, France). Journal of Structural Geology 14, 461–474.

Averbuch, O., Frizon de Lamotte, D., Kissel, C., 1993. Strain distribution above a lateral culmination: an analysis using microfaults and magnetic fabric measurements in the Corbières thrust belt (NE Pyrenees, France). Annales Tectonicae VII, 3–21.

Averbuch, O., Mattei, M., Kissel, C., Frizon de Lamotte, D., Speranza, F., 1995. Cinématique des déformations au sein d'un système chevauchant aveugle: l'exemple de la Montagna dei Fiori (front des Apennins centraux, Italie). Bulletin de la Société Géologique de France 166, 451–461.

Averbuch, O., Mansy, J-L., Lamarche, J., Lacquement, F., Hanot, F., 2004. Geometry and kinematics of the Boulonnais fold-and-thrust belt (N France): implications for the dynamics of the Northern Variscan thrust front. Geodinamica Acta 17/2, 163–178.

Bayona, G., Thomas, W.A., Van der Voo, R., 2003. Kinematics of thrust-sheets within transverse zones: a structural and paleomagnetic investigation in the Appalachian thrust belt of Georgia and Alabama. Journal of Structural Geology 25, 1193–1212.

Borradaile, G.J., Henry, B., 1997. Tectonic applications of magnetic susceptibility and its anisotropy. Earth Science Reviews 42, 49–93.

Borradaile, G.J., Tarling, D.H., 1981. The influence of deformation mechanisms on magnetic fabric in weakly deformed rocks. Tectonophysics 77, 151–168.

Boulvain, F., Coen-Aubert, M., 1997. Le sondage de Focant: lithostratigraphie et implications structurales, Memoirs of the Geological Survey of Belgium, vol. 43 1997. 74pp.

Butler, R., 1982. Hanging wall strain: a function of duplex shape and footwall topography. Tectonophysics 88, 235–246.

Calassou, S., Larroque, C., Malavieille, J., 1993. Transfer zones of deformation in thrust wedges: an experimental study. Tectonophysics 221, 325–344.

Cobbold, P.R., Durand, S., Mourgues, R., 2001. Sandbox modeling of thrust wedges with fluid-assisted detachments. Tectonophysics 334, 245–258.

Coward, M.P., Potts, G.J., 1983. Complex strain patterns developed at the frontal and lateral tips to shear zones and thrust zones. Journal of Structural Geology 5, 383–399.

Dahlstrom, C.D.A., 1970. Structural geology in the eastern margin of the Canadian Rocky Mountains. Bulletin of Canadian Petroleum Geology 18, 332–406.

Dixon, J.M., Liu, S., 1992. Centrifuge modeling of the propagation of thrust faults. In: McClay, K.R. (Ed.), Thrust Tectonics. Chapman and Hall, London, pp. 53–69.

Donzeau, M., Gamond, J.-F., Mugnier, J.-L., 1993. Evolution latérale et amortissement d'une structure chevauchante, un exemple du Nord Vercors. Compte Rendus Geosciences Paris 317, 1675–1682.

Franke, W., 2000. The mid-European segment of the Variscides: Tectonostratigraphic units, terrane boundaries and plate tectonic evolution. In: Franke, W., Haak, V., Oncken, O., Tanner, D. (Eds.), Orogenic Processes: Quantification and Modeling in the Variscan Belt Geological Society of London Special Publication, vol. 179, pp. 35–61.

Frizon de Lamotte, D., Guezou, J-C., Averbuch, O., 1995. Distinguishing lateral folds in thrust-systems: examples from Corbières (SW France) and Betic Cordilleras (SE Spain). Journal of Structural Geology 17, 223–244.

Goudalier, M., 1998. Dolomitisation de calcaires du Frasnien moyen de la Belgique: contrôle sédimentaire, diagénétique et tectonique. PhD thesis, Université de Lille 1, France.

Han, G., Yans, J., Goudalier, M., Lacquement, F., Corfield, R.M., Mansy, J.-L., Boulvain, F., Préat, A., 2003. Recognition and implication of tectonic loading-induced reheating in the northern Variscan front (Belgium and northern France), based on an illite Kübler index and oxygen isotope study. International Journal of Earth Science 92, 348–363.

Henry, P., Le Pichon, X., 1991. Fluid flow along a décollement layer: a model applied to the 16°N section of the Barbados accretionary wedge. Journal of Geophysical Research 96, 6507–6528.

Holl, J.E., Anastasio, D.J., 1995. Kinematics around a large-scale oblique ramp, southern Pyrenees, Spain. Tectonics 14, 1368–1379.

Hollmann, G., Von Winterfeld, C., 1999. Laterale strukturvariationen eines Vorlandüberschiebungs-gürtels. Zeitschrift der Deutschen Geologischen Gesellschaft 150, 431–450.

Housen, B.A., Richter, C., Van der Pluijm, B.A., 1993. Composite magnetic anisotropy fabrics: experiments, numerical models and implications for the quantification of rock fabrics. Tectonophysics 220, 1–12.

Hyett, A.J., 1990. Deformation around a thrust tip in Carboniferous limestone at Tutt Head, near Swansea, south Wales. Journal of Structural Geology 12, 47–58.

Jelinek, V., 1981. Characterization of the magnetic fabric of rocks. Tectonophysics 79, 63–67.

Kligfield, R., Owens, W.H., Lowrie, W., 1981. Magnetic susceptibility anisotropy, strain and progressive deformation in Permian sediments from the Maritime Alps (France). Earth and Planetary Science Letters 55, 181–189.

Lacquement, F., 1997. Retraitement du profil sismique M146, nord de de la France. Unpublished report, Compagnie Générale de Géophysique-Université de Lille.

Lacquement, F., 2001. L'Ardenne Varisque. Déformation progressive d'un prisme sédimentaire pré-structuré, de l'affleurement au modèle de chaîne. Publication de la Société Géologique du Nord 29.

Lacquement, F., Mansy, J.-L., Hanot, F., Meilliez, F., 1999. Retraitement et interprétation d'un profil sismique pétrolier méridien au travers du massif paléozoïque ardennais (nord de la France). Compte Rendus Geosciences Paris 329, 471–477.

Ledru, P., Faure, M., Bouchot V., 2001. Le Massif Central, témoin de la chaîne varisque ouest européenne. In: Géologue, Spécial Massif Central, no. 130–131, pp. 30–44.

Liu Huiqi, McClay, K.R., Powell, D., 1992. Physical models of thrust wedges. In: McClay, K.R. (Ed.), Thrust Tectonics. Chapman and Hall, London, pp. 71–81.

Macedo, J., Marshak, S., 1999. Controls on the geometry of fold–thrust belt salients. Geological Society of America Bulletin 111, 1808–1822.

Mansy, J.-L., Everaerts, M., De Vos, W., 1999. Structural analysis of the adjacent Acadian and Variscan fold belts in Belgium and northern France from geophysical and geological evidence. Tectonophysics 309, 99–116.

Marshak, S., Wilkerson, M.S., Hsui, A.T., 1992. Generation of curved fold–thrust belts: insight from simple physical and analytical models. In: McClay, K.R. (Ed.), Thrust Tectonics. Chapman and Hall, London, pp. 83–92.

Marton, E., Mansy, J.L., Averbuch, O., Csontos, L., 2000. The Variscan belt of Northen France–Southern Belgium: geodynamic implications of new paleomagnetic data. Tectonophysics 324, 57–80.

Meilliez, F., André, L., Blieck, A., Fielitz, W., Goffette, O., Hance, L., Khatir, A., Mansy, J.L., Overlau, P., Verniers, J., 1991. Ardenne-Brabant. Sciences Géologiques Bulletin 44, 3–29.

Molina-Garza, R., Zijderveld, J.D.A., 1996. Paleomagnetism of Paleozoic strata, Brabant and Ardennes Massifs, Belgium: implications of prefolding and postfolding late Carboniferous secondary magnetizations for European apparent polar wander. Journal of Geophysical Research 101 (B7), 15779–15818.

Oncken, O., Plesch, A., Weber, J., Ricken, W., Schrader, S., 2000. Passive margin detachment during arc-continent collision (Central European Variscides). In: Franke, W., Haak, V., Oncken, O., Tanner, D. (Eds.), Orogenic Processes: Quantification and Modeling in the Variscan Belt Geological Society of London Special Publications, vol. 179, pp. 199–216.

Parès, J.M., van der Pluijm, B.A., Dinarès-Turell, J., 1999. Evolution of magnetic fabrics during incipient deformation of mudrocks (Pyrenees, northern Spain). Tectonophysics 307, 1–14.

Paulsen, T., Marshak, S., 1999. Origin of the Uinta recess, Sevier fold–thrust belt, Utah: influence of basin architecture on fold-thrust belt geometry. Tectonophysics 312, 203–216.

Philippe, Y., 1995. Rampes latérales et zones de transfert dans les chaînes plissées: géométrie, conditions de formation et pièges structuraux associés. PhD thesis, Université de Savoie, France.

Raoult, J.-F., 1986. Le front varisque du Nord de la France d'après les profils sismiques, la géologie de surface et les sondages. Revue de géologie dynamique et de géographie physique 27, 247–288.

Robion, P., Averbuch, O., Sintubin, M., 1999. Fabric development and metamorphic evolution of the Paleozoic slaty rocks from the Rocroi massif (French–Belgian Ardennes): new constrains from magnetic fabrics, phyllosilicate preferred orientation and illite crystallinity. Tectonophysics 309, 257–273.

Rochette, P., Jackson, J., Aubourg, C., 1992. Rock magnetism and the interpretation of anisotropy of magnetic susceptibility. Review of Geophysics 30, 209–226.

Schirmer, T.W., 1988. Structural analysis using thrust-fault hanging-wall sequence diagrams: Ogden duplex, Wasatch Range, Utah. American Association of Petroleum Geologists Bulletin 72, 573–585.

Szaniawski, R., Lewandowski, M., Mansy, J.-L., Averbuch, O., Lacquement, F., 2003. Syn-folding remagnetization events in the French–Belgium Variscan thrust front as markers of the fold-and-thrust belt kinematics. Bulletin de la Société Géologique de France 174, 511–523.

Tarling, D.H., Hrouda, F., 1993. The Magnetic Anisotropy of Rocks. Chapman and Hall, London. 217pp.

Tavarnelli, E., 1996. Ancient synsedimentary structural control on thrust ramp development; an example from the Northern Apennines. Terra Nova 8, 65–74.

Thomas, W.A., 1990. Controls on locations of transverse zones in thrust belts. Eclogae Geologicae Helvetica 83, 727–744.

Van der Voo, R., 1993. Paleomagnetism of the Atlantic, Tethys and Iapetus Oceans. Cambridge University Press, Cambridge. 411pp.

Wilkerson, S., Apotria, T., Farid, T., 2002. Interpreting the geologic map expression of contractional fault-related fold terminations: lateral/oblique ramps versus displacement gradients. Journal of Structural Geology 24, 593–607.

Wiltschko, D.V., Eastman, D.B., 1982. Role of basement warps and faults in localizing thrust-fault ramps. Geological Society of America Memoir 158, 177–190.

Zegers, T., Dekkers, M.J., Bailly, S., 2003. Late Carboniferous to Permian remagnetization of Devonian limestones in the Ardennes: role of temperature, fluids and deformation. Journal of Geophysical Research 108 (B7), 2357.